Electronic Configuration of High-Spin Imidazole-Ligated Iron(II) Octaethylporphyrinates

ARTICLE *in* INORGANIC CHEMISTRY · JUNE 2006

Impact Factor: 4.76 · DOI: 10.1021/ic052194v · Source: PubMed

Published in final edited form as:
Inorg Chem. 2006 May 15; 45(10): 4177–4185.

Electronic Configuration of High-Spin Imidazole-Ligated Iron(II) Octaethyl-porphyrinates

Chuanjiang Hu[†], **An**[†], **Bruce C. Noll**[†], **Charles E. Schulz**[‡,*], and **W. Robert Scheidt**[†,*]

Abstract

The preparation and characterization of two new five-coordinate, imidazole- ligated, high-spin iron (II) octaethylporphyrinates is described. [Fe(OEP)(1,2-Me_2Im)] and [Fe-(OEP)(2-MeHIm)] have been characterized by X-ray structure determinations and temperaturedependent Mössbauer spectroscopy in zero and applied magnetic field. The distinction between imidazole-ligated and other ligands in high-spin iron(II) porphyrinates, noted for a series of tetraarylporphyrinate derivatives (Hu, et al. JACS 2005, *127*, 5675), is seen here as well. The sign of the quadrupole splitting constant is again negative, which is unique to the imidazole derviatives and suggests a distinct electronic structure. The derivatives again display a remark-able temperature dependence in the quadruple splitting, which is also seen for dexoymyoglobin and -hemoglobin. Structural features for the two new derivatives are similar to those seen earlier, although the core conformations show somewhat more doming character.

Introduction

Iron porphyrinate complexes (hemes) are the active sites in many biologically important systems. Knowledge of both the electronic and geometric structure at iron appears to be the key to understanding the diverse and complicated functions of these hemoproteins. Indeed, the electronic ground states of models of these iron(II) species have been intensively investigated both experimentally and theoretically and yet are far from being known with certainty.

The best known heme-based systems are the O_2-binding proteins myoglobin and hemoglobin, which shuttle between deoxy and oxy states. The iron of the heme remains in the 2+ formal oxidation state. In the deoxy state, iron(II) is five-coordinate and bound to the protein by the proximal histidine ligand. The heme becomes six-coordinate upon binding an O_2molecule. The structural changes that accompany this spin state change are essential to the mechanism of cooperative O_2-binding by hemoglobin and are the basis of the T → R transition of hemoglobin.[1-3] In brief, the five-coordinate deoxy heme has a structure with a significant displacement of the iron atom out of the heme plane whereas the six-coordinate oxyheme has the iron in the plane. The signaling of the binding state between the four hemes of tetrameric hemoglobin as dioxygen is bound forms the basis of the cooperativity and is strongly coupled to the structure of the five-coordinate iron(II) porphyrin sites.

[†]University of Notre Dame
[‡]Knox College
[*]To whom correspondence should be addressed

Supporting Information Available: Figures S1 and S2 show ORTEP diagrams of [Fe(OEP)(1,2-Me^2Im)] and [Fe(OEP)(2-MeHIm)]. Figure S3 displays displacements form the N_4plane. Figures S4 and S5 show the simultaneous fits to the variable field Mössbauer data. Tables S13 and S14 give full details on the observed data and the fits. Tables S1-S12 give complete crystallographic details, atomic coordinates, bond distances and angles, anisotropic temperature factors, and fixed hydrogen atom positions for [Fe(OEP)(1,2-Me_2Im)] and [Fe-(OEP)(2-MeHIm)]. This information is available as a PDF file. The crystallographic information files (CIF) are also available. This material is available free of charge via the Internet at http://pubs.acs.org.

The structures of several high-spin imidazole-ligated iron(II) porphyrinates have been determined by X-ray crystallography.[4-7] Several common features are expected and observed - an expanded porphinato core, large equatorial Fe-N_p[8] bond distances and a large out-of-plane displacement of the iron(II) atom. Perhaps somewhat unexpectedly, there are large variations in the nature of the core conformation ranging from strongly domed structures to saddled and folded cores. These lead to substantial variations (0.38 to 0.55 Å) in the magnitude of the out-of-plane displacements of iron from the 24-atom porphyrin core. However, the iron displacements from the four nitrogen atom plane are much more invariant at 0.36 Å.

The electronic structure of iron(II) hemes is quite challenging to study because most spectroscopic probes provide little or no information about the states of the d^6metal ion. The difficulty in understanding the electronic structure of the five-coordinate imidazole-ligated hemes is reflected in both the relatively large amount published on the issue and some changing interpretations for both experimental and theoretical studies. A number of recent density functional theory (DFT) studies for five-coordinate imidazole-ligated hemes have appeared.[9-12] However, the conclusions reached about the electronic ground state are by no means uniform. Three of the four DFT calculations found that a triplet state was lower in energy than the experimentally observed quintet state. In all of these cases, a quintet state is predicted to be lowest in energy when the iron(II) atom is constrained to be further out of the porphyrin plane than the value obtained for the triplet state. In other words, DFT calculations suggest that large values ofΔFe stabilize higher spin multiplicities. A fourth study [11] does predict a quintet ground state.

Iron(II) is a non-Kramers system and, except in fortuitous circumstances is EPR silent. Fortunately, Mössbauer spectroscopy has proven to be an extremely useful spectroscopic probe for the electronic structure of iron(II). As part of a more general program of characterization of high-spin iron(II) porphyrinates, our previous study[4] reported detailed Mössbauer spectra in applied magnetic field for six new derivatives. The Mössbauer data measured all high-spin iron(II) samples in both zero and applied magnetic field, along with previously studied porphyrin derivatives, showed the same Mössbauer behavior (negative quadrupole splitting values that are strongly temperature dependent) as those of deoxymyoglobin and deoxyhemoglobin, which indicates they have the same electron configuration. The electronic structure implied by the Mössbauer results shows that all of these deoxymyoglobin models are distinctly di erent from those of high-spin iron(II) porphyrinates ligated by all other axial ligands.

In this paper, we have examined *β*-substituted octaethylporphyrin derivatives rather than tetraaryl-substituted species. One of our goals was to examine whether the β-substituted porphyrins display any significant di erence from the tetraaryl derivatives previously characterized. We have synthesized two new five-coordinate iron(II) octaethylporphyrinates using hindered imidazoles as the axial ligand. We report the molecular structures and further examine their electron configuration and the structural di erence caused by the change of the porphyrin (from tetraarylporphyrins to octaethylporphyrins).

Experimental Section

General Information. All reactions and manipulations for the preparation of the iron(II) porphyrin derivatives were carried out under argon using a double-manifold vacuum line, Schlenkware, and cannula techniques. Toluene and hexanes were distilled over sodium benzophenone ketyl. Ethanethiol (Aldrich) was used as received. 2-Methylimidazole and 1,2-dimethylimidazole were purchased from Aldrich, recrystallized from toluene, and dried under vacuum. The free-base porphyrin octaethylporphyrin (H_2OEP)8 was purchased from Midentury. The metallation of the free-base porphyrin to give [Fe(OEP)Cl] was done as

previously described.[13] $[Fe(OEP)]_2O$ was prepared according to a modified Fleischer preparation.[14]

Mössbauer measurements were performed on a constant acceleration spectrometer from 4.2 K to 300 K with optional small field and in a 9 T superconducting magnet system (Knox College). Samples for Mössbauer spectroscopy were prepared by immobilization of ground crystalline material in Apiezon M grease.

Synthesis of [Fe(OEP)(1,2-Me_2Im)] and [Fe(OEP)(2-MeHIm)]. [Fe^{II}(OEP)] was prepared by reduction of $[Fe(OEP)]_2O$ (0.04 mmol) with ethanethiol (1 mL) in toluene (15 mL). The toluene solution was stirred until the color turned dark red. Solvent was removed under vacuum. Excess ligand (1,2-dimethylimidazole or 2-methylimidazole) (0.4 mmol) in toluene (15 mL) was added via cannula transfer to the solid [Fe(II)(OEP)] and stirred for 1 hour. X-ray quality crystals were obtained in 8 mm × 250 mm sealed glass tubes by liquid di usion using hexanes as nonsolvent.

X-ray Structure Determinations. Single crystal experiments were carried out on a Bruker Apex system with graphite monochromated Mo-K radiation (λ = 0.71073 Å). The crystalline samples were placed in inert oil, mounted on a glass pin, and transferred to the cold gas stream of the di ractometer. Crystal data were collected at 100 K. The structures were solved by direct methods using SHELXS-97 [15] and refined against F_2using SHELXL-97;[16,17] subsequent difference Fourier syntheses led to the location of the remaining non-hydrogen atoms. For the structure refinement all data were used including negative intensities. All nonhydrogen atoms were refined anisotropically if not remarked otherwise below. For methyl hydrogen atoms of an imidazole, a di erence electron density synthesis is calculated around the circle which represents the loci of possible hydrogen positions (for a fixed C-H distance and X-C-H angle). The maximum electron density (in the case of a methyl group after local threefold averaging) is taken as the starting hydrogen position. Then the hydrogen coordinates are re-idealized and 'ride' on the atoms to which they are attached with fixed thermal parameters (u_{ij}= 1.5U_{ij}(eq)). Other hydrogen atoms were placed at idealized positions and a riding model (u_{ij}= 1.2U_{ij}(eq)) was used for subsequent refinements. The program SADABS [18] was applied for the absorption correction. Brief crystal data for both structures are listed in Table1. Complete crystallographic details, atomic coordinates, anisotropic thermal parameters, and fixed hydrogen atom coordinates are given in the Supporting Information for both structures.

[Fe(OEP)(1,2-Me_2Im)]. $0.97C_6H_5CH_3$. A red crystal with the dimensions 0.2×0.1×0.05 $mm^3$was used for the structure determination. The asymmetric unit contains one porphyrin complex and one partially occupied toluene molecule. During the refinement, one di erence density peak at ~2.0 e/$Å^3$, 1.1 ÅA away from Fe(1a), and on the opposite side of the porphyrin plane was identified. It was refined as a disordered minor iron (Fe(1b)). Because the occupancy is very small (~3%), the 2-methylimidazole coordinated to Fe(1b) was not located. To accommodate this model, the imidazole and toluene solvent were both refined at the same occupancy as the major iron. The anisotropic displacements of both iron atoms are restrained to be the same. After the final refinement, the occupancy of the major iron, imidazole and toluene solvent was found to be 97%.

[Fe(OEP)(2-MeHIm)].$C_6H_5CH_3$. A red crystal with the dimensions 0.46 × 0.11 × 0.06 $mm^3$was used for the structure determination. The 2-methylimidazole was found to be disordered over two positions, a major and a minor position. The minor 2-methylimidazole was refined as a rigid group, the thermal displacement parameters of N(5b) and N(6b) were each constrained to be equal to the anisotropic displacement parameters of the corresponding atoms N(5a) and N(6a) of the major imidazole orientation. After the final refinement the

occupancy of the major imidazole orientation was found to be 75%. The asymmetric unit also contains one fully occupied toluene molecule.

Results

The two new five-coordinate imidazole-ligated iron(II) octaethylporphyrin complexes were synthesized starting from the iron(III) μ-oxo derivative ([Fe(OEP)]$_2$O). Ethanethiol reduction to give the iron(II) species [Fe(OEP)] was followed by reaction with a hindered imidazole ligand. Crystalline samples suitable for X-ray structure determinations were obtained by liquid diffusion of a nonsolvent layered above the porphyrin solution in sealed glass tubes. The structures of two derivatives have been obtained: [Fe(OEP)(1,2-Me$_2$Im)] and [Fe(OEP)(2-MeHIm)].

An ORTEP diagram of [Fe(OEP)(1,2-Me$_2$Im)] is illustrated in Figure 1. The major iron and 2-methylimidazole (97% occupancy) are shown. The dihedral angle ϕ between the imidazole plane and the plane defined by N(4), Fe(1a), N(5) is 10.5°. The dihedral angle between the imidazole ligand and the 24-atom mean porphyrin plane is 89.5°. An ORTEP diagram showing both positions of the iron atom is provided in Figure S1.

An ORTEP diagram of [Fe(OEP)(2-MeHIm)] is given in Figure 2. The imidazole ligand is disordered over two positions with a major and a minor orientation. The diagram shows the major orientation (75% occupancy) of the axial ligand. An ORTEP diagram showing both orientations of the axial ligand is provided in Figure S2. The labeling scheme is consistent with all of the diagrams and tables. The dihedral angle between the two orientations of the imidazole ligand is 6.6°. Although the imidazole ligand of this structure is disordered, the major orientation of the ligand dominates the structural features of the molecule. The dihedral angle (ϕ) between the major imidazole ligand and the plane defined by N(1), Fe, N(5a) is 19.5°. The dihedral angle between the major imidazole ligand and the 24-atom mean porphyrin plane is80.9°. Other selected geometric parameters involving the iron and imidazole ligand are given in Table 2 for both complexes.

Illustrated in Figure 3 are formal diagrams of the porphyrin cores of the two new iron(II) imidazole structures that gives the displacements of each atom from the mean plane of the 24-atom porphyrin core in units of 0.01 Å. The orientation of the imidazole ligand with respect to the core atoms is shown by the line with the circle representing the methyl group bound at the 2-carbon position. An analogous diagram showing atomic displacements from the mean plane of the four nitrogen atoms is given in Figure S3. Also included on the diagrams of Figure 3 are the individual Fe-N$_p$bond lengths. The average Fe-N$_p$bond lengths are 2.080(6) ÅA for [Fe(OEP)(1,2-Me$_2$Im)] and 2.077(7) ÅA for [Fe(OEP)(2-MeHIm)] . These average values and other selected bond distances and angles are given in Table 2. A complete listing of bond distances and angles for both structures is given in the Supporting Information.

The Fe-N(imidazole) bond lengths are 2.171(3) and 2.135(3) Å, respectively, which are similar to those in iron(II) tetraarylporphyrinates. In both structures the imidazole ligand Fe-N bond vector is tilted off the normal to the 24-atom porphyrin mean plane. The value of the tilt angle, given by Θ in Table 2, is 6.9°for [Fe(OEP)(1,2-Me$_2$Im)] and 3.8°for [Fe(OEP)-(2-MeHIm)]. Two other important angles associated with the imidazole ligands (Fe-N-C) are given in Table 2. The displacements of the iron atom out of the porphyrin plane are 0.37 and 0.34 Å, respectively. The radii of the porphyrin cores, given by Ct…N in Table 2, are nearly identical at 2.047 and 2.049 Å.

These crystalline species were studied with variable temperature Mössbauer spectroscopy.Both the quadrupole splitting and isomer shift values show strong temperature dependence. The quadrupole splitting for the crystalline species [Fe(OEP)(2-MeHIm)] at 4.2 K is 1.94 mm/s

and at 298 K is 1.34 mm/s. The isomer shifts at these respective temperatures are 0.93 and0.82 mm/s. At 4.2 K the quadrupole splitting for [Fe(OEP)(1,2-Me_2Im)] is 2.19 mm/s and the isomer shift is 0.92 mm/s. These values at 298 K are 1.59 mm/s and 0.80 mm/s respectively. Mössbauer parameters at various temperatures between 4.2 K and 298 K are given in Table S13 of the Supporting Information.

Discussion

As noted in the Introduction, we have previously investigated the molecular structures and electron configuration of five-coordinate high-spin imidazole-ligated iron(II) tetraarylporphyrinates as deoxyheme model compounds.[4,5] These complexes have several common features including an expanded porphinato core, large equatorial Fe-$N_p$bond distances and a significant out-of-plane displacement of the iron(II) atom. But they also show much variation in core conformation as well as di erences in the orientation of imidazole plane with respect to the porphyrin core. Mössbauer spectra shows a negative sign for the quadrupole splitting and a strong temperature-dependence that suggests that they all have the same unusual electronic ground state as deoxyhemoglobin and deoxymyoglobin. In this paper, we explore the possible e ects of di erent substituents of the porphyrin core (β-pyrrole substituents vs. *meso*-aryls) on the electron configuration and on any structural di erences, especially core conformations. Accordingly, we have synthesized two new five-coordinate iron(II) octaethylporphyrinates with sterically hindered 2-methylimidazole and 1,2-dimethylimidazole as ligands [27] and characterized them by X-ray crystallography and Mössbauer spectroscopy.

Molecular Structures. The overall structural features of [Fe(OEP)(1,2-Me_2Im)] and [Fe-(OEP)(2-MeHIm)] are those expected for high-spin iron(II) porphyrinates.[4,28] Selected structural data for these two complexes are given in Table 2 and full structural information is given in the Supporting Information. Also given in Table 2 are the values found for a number of previously characterized high-spin iron(II) systems. The average Fe-$N_p$bond distance for [Fe(OEP)(1,2-Me_2Im)] (2.080(6) Å) and [Fe(OEP)(2-MeHIm)] (2.077(7) Å) are well within the range for the other imidazole-ligated porphyrinates (2.073 ÅA to 2.087 Å). The axial Fe-N_{Im}bond length is 2.171(3) ÅA in [Fe(OEP)(1,2-Me_2Im)] and 2.135(3) in [Fe(OEP)(2-MeHIm)], which is in the range for those of the tetraarylporphyrinates. The Fe-N_{Im}bond lengths for the imidazole-ligated structures show a small but significant variation. The small variation is no doubt a consequence of the hindering methyl group and to di erences in relative orientation of the axial ligand and di ering core conformations.

Similarly, the displacement of the iron atom from the plane of the four nitrogen atoms (ΔN_4) is 0.37 ÅA for [Fe(OEP)(1,2-Me_2Im)] and 0.34 ÅA for [Fe(OEP)(2-MeHIm)], values that bracket the average for the tetraaryl derivatives (Table 2). The displacements of iron from the 24-atom porphyrin plane (Δ) are 0.45 and 0.46 Å, respectively. The di erence between the two values (note that Δ is larger than Δ N_4) is a measure of porphyrin core doming. The two complexes both have a moderate (0.08 and 0.12 Å) domed conformation. Porphyrin core doming is frequently observed for metalloporphyrin derivatives with metal ions that are too large to fit into the central hole of the porphyrin ring,[29] but doming is not as prevalent as might have been expected in the imidazole-ligated iron(II) species.

The large iron(II) ion is accommodated in the central hole of the porphyrin ring not only by the large iron atom displacements and long Fe-$N_p$bond distances but also by a radial expansion of the core (an increase in the size of the central hole).[30] The radius of the central hole is 2.047 or 2.049 ÅA for these two new imidazole-ligated porphyrinates, values similar to those of the tetraarylporphyrinates.

The steric bulk of the 2-methyl group leads to, in all derivatives examined to date, an off-axis tilt of the axial Fe-$N_p$bond and a rotation of the imidazole ligand that leads to unequal Fe-

N_{Im}-C_{Im}angles. Values for iron(II) imidazole species are given in Table 2. These angles have an average value of 131.4°on the methyl side and 122.7°on the other side. The off-axis tilt and imidazole rotation are correlated so as to maximize the distance between the 2-methyl group and porphyrin core atoms. The ORTEP drawings of Figures 1 and 2 clearly show that the axial Fe-N_{Im}bond vector is tilted from the heme normal. The tilt angles are 3.8 and 6.9°. As seen in Table 2, the small di erences in ligand tilting appears not to be correlated with any other structural feature, showing no apparent relation to varying core conformation or the orientation of the axial ligand plane with respect to Fe-$N_p$directions.

There is an interesting pattern in Figure 3, comparing [Fe(OEP)(1,2-Me_2Im)] with [Fe(TPP)-(2-MeHIm)](2-fold). Both have small dihedral angles (ϕ) which are around 10°. The corresponding Fe-$N_p$distances close to the imidazole plane are longer than the other pair as given in Figure 3 and the corresponding Fe-N_{im}distances (2.171(3) ÅA and 2.161(5) Å) are also longer than those in other porphyrinates with larger dihedral angles (ϕ). Both longer Fe-$N_p$and Fe- N_{im}distances are related to the smaller *Å* probably due to the interaction between the imidazole ligand and the porphyrin core.

Although these structural features are a result of the large size of the high-spin iron(II) ion, an examination of these iron(II) values in Table 2 shows that there is some variation within the set of high-spin five-coordinate iron(II) derivatives. Core conformations of the nine five-coordinate high-spin iron(II) porphyrinates are illustrated in Figure 4. Displayed in linear fashion are the displacements of the iron atom and the 24 atoms of the porphyrin core from the four pyrrole nitrogen mean plane. The two OEP structures are at the top, the remaining structures are grouped by similar overall conformation and the hybrid porphyrin structure is shown last. The orientation of the imidazole ligand with respect to the porphyrin core is also shown: the vertical line represents the position of the imidazole shown with the pyrrole closest to the 2-methyl group. When there is a minor orientation this is illustrated with a second vertical line; the major orientation is always shown to the left. With the exception of the [Fe(TPP)(2-MeHIm)](twofold) structure, which has two equivalent orientations of the axial ligand, it is expected that the major ligand orientation dominates the observed structure. The results summarized in Figure 4 make evident that there is not a *single* preferred conformation for imidazole-ligated high-spin iron(II) complexes. There are some similarities in the tetraaryl complexes as we discussed in a previous study.4 Both of the OEP complexes have an obvious domed conformation, which is similar to that of [Fe(TPP)(2-MeHIm)][19] and [Fe(TTP)(2-MeHIm)].[4]

The core conformations have also been analyzed by the normal structural decomposition (NSD) method provided by Shelnutt et al.[31,32] Table 3 lists the out-of-plane displacements of the minimal basis for the nine five-coordinate high-spin iron(II) porphyrinates. NSD also shows wide variation of the core conformations from saddling to doming to waving. The doming deformation is the largest component for the two OEP complexes as shown in Table 3. Although a number of the tetraaryl derivatives also have a substantial doming deformation, it is not as prominent as those of the two OEP derivatives. The doming displacements in the 1,2-dimethylimidazole-ligated complexes are smaller than those in the corresponding 2-methylimidazole complexes and may be a result of the (small) steric di erences between two ligands. However, the TPP complexes do not fit this pattern. The di erent core conformations for di erent crystalline forms of the TPP complexes suggest that solid-state packing and solvates in solid state will also influence the core conformation. Other weak interactions in the solid state, such as π-π interactions and hydrogen bonding, are also possible factors.

Electronic Structure. The electronic structure of these two new complexes has also been studied by Mössbauer spectroscopy. Mössbauer isomer shifts (δ) and quadrupole splitting (ΔE_Q) values have been measured from room temperature to 4.2 K. The values of $E_Q$observed at 4.2

K are 1.94 and 2.19 mm/s, for [Fe(OEP)(1,2-Me_2Im)] and [Fe(OEP)(2-MeHIm)], respectively. These are within the range of previously reported high-spin iron(II) species;[4,33] the large value of the isomer shift (~0.9 mm/s) is consistent with high-spin iron(II).[34] For comparison, the Mössbauer data for these two complexes and related species are listed in Table4. From these data, as outlined below, it is almost certain that all of these five-coordinate imidazole-ligated species share many common electronic structure features.

There is a substantial temperature variation of the quadrupole splitting values; complete values of δ and ΔE_Qvs. T are tabulated in Table S13. A plot of the data for these two complexes and related species is given in Figure 5. The value of ΔE_Qdecreases significantly as the temperature is increased. The observed temperature dependence of $\Delta E_Q$for these two new porphyrinates is similar to the variation seen (over a smaller temperature range) for deoxymyoglobin and -hemoglobin samples[33,38,39,40] and for those of the tetraarylporphyrinate derivatives.[4,20] As discussed previously,[4] the explanation for this temperature variation is that there are close-lying excited states. The excited states could have the same or di ering spin multiplicity relative to the ground state.

The application of applied magnetic field Mössbauer spectroscopy provides more detailed information concerning the electronic ground states. The Mössbauer data in strong magnetic fields shown in Figure 6 were fit with the spin Hamiltonian model used by Kent et al. [33]

$$H = D\left[S_z^2 - 1/3\,S(S+1)\right] + E\left(S_x^2 - S_y^2\right) + \vec{H}\cdot\tilde{g}\cdot\vec{S} + H^Q - g_N^*\beta_N\vec{H}\cdot\vec{I} + \vec{S}\cdot\tilde{A}^*\cdot\vec{I}$$

where D and E are the axial and rhombic zero-field splitting parameters that describe the fine structure of the $S = 2$ multiplet,$\tilde{A}^*$ is the magnetic hyperfine tensor and H^Qgives the nuclear quadrupole interaction:

$$H^Q = \frac{eQV_{zz}}{12}\left[3I_z^2 - I(I+1) + \eta\left(I_x^2 - I_y^2\right)\right]$$

Q is the quadrupole moment of the ^{57}Fe nucleus and $\eta = (V_{xx}\text{-}V_{yy})/V_{zz}$, where $V_{ii}$are components of the electric field gradient. The quadrupole splitting and isomer shift were constrained to the values determined from the zero-field data.

An analysis of the spectra showed the largest component of the electric field gradient, V_{zz}, to have a negative value and hence the sign of the quadrupole splitting value is also negative. The asymmetry parameters for two new complexes are relatively large, 0.43 and0.26, which are consistent with other related imidazole-ligated species.[4,33,38-40] The large asymmetry parameter indicates the low symmetry of the electric field gradient (EFG), which is also reflected in the solid-state structures of these complexes.

As shown in Table 4, there are a number of five-coordinate high-spin iron(II) porphyrinate derivatives definitely known[35-37] to have a positive value of the quadrupole splitting, while the positive value of a number of others must be regarded as highly probable.[21,22,23,35] These derivatives are listed in Table 4 with a "+" sign. As shown in the table, all of these complexes have an anionic species as the axial ligand.

For an iron compound with nonionic ligands, it is reasonable to assume that the EFG at the nucleus is dominated by contributions from the d-electrons. Following the discussion of Debrunner,[34] a large positive quadrupole splitting with a small asymmetry parameter is consistent only with the doubly occupied d orbital being in the heme plane, i.e., the orbital must be either d_{xy}or d_{x^2}-$_{y^2}$ The$(d_{xy}^2)(d_{xz})^1(d_{yz})^1(d_{z^2})^1(d_{x^2}\text{-}_{y^2})$ ground state has also been assigned for [Fe(TPP)(OPh)]-[36] and Na(222)[Fe(OAc)(TpivPP)].[37] Indeed, we believe that

the$(d_{xy}^2)(d_{xz})^1(d_{yz})^1(d_z^2)^1(d_{x^2-y^2})$state is the usual one for high-spin iron(II) porphyrinates; the"unusually large" quadrupole split doublet signal from high-spin iron(II) should be regarded as normal.

The negative sign for the quadrupole splitting value usually indicates that the more negative charge is along the heme normal, which led to the conclusion that the doubly occupied d orbital for the imidazole complexes is a $d_\pi$orbital, i.e., the doubly occupied orbital is perpendicular to the heme plane. But in these imidazole-ligated complexes, the negative quadrupole splitting associated with large asymmetric parameters make this conclusion unclear. The $d_{xz}$and d_{yz}orbitals have an EFG with a negative component V_{zz}along the heme normal. So if the doubly-occupied d orbital is due to a low-symmetry ligand field, a mixture of the d_{xz}, $d_{yz}$and d_{xy}orbitals can give a negative sign to ΔE^Q, and the asymmetry parameters can be rel- atively large. In this model, when $\Delta E_Q$is negative, the largest component of the EFG will no longer lie near the heme normal. Indeed, single crystal Mössbauer data have shown that for deoxymyoglobin, $V_{zz}$is negative and far from the heme normal, within 22°of the heme plane.[38] So, the Mössbauer properties are better described by a hybrid orbital comprised of the two axial $d_\pi$orbitals, along with a significant d_{xy}contribution. Such mixing of $d_{xy}$with the $d_\pi$orbitals will occur in any ligand field of su ciently low symmetry. For example, an axial potential rotated o an octahedral symmetry axis will mix the states. Such a field would be expected for 5-coordinate hemes with the axial ligand displaced from the heme normal. A detailed analysis of the Mössbauer spectra of all high-spin iron(II) porphyrinates is in progress, and will be published subsequently.[41]

We believe that it is the low-symmetry, mixed d-orbital configuration with a ΔE_Qthat is smaller and negative, as found for deoxymyoglobin, deoxyhemoglobin and the imidazole-ligated iron (II) porphyrinates that is the unusual electronic state for high-spin iron(II) porphyrinates. Thus, high-spin iron(II) porphyrinates can be divided into two di erent electronic configurations. As can be seen from a comparison of structural data (Table 2) with the signed quadrupole derivatives of Table 4, this division into two groups is also manifested in the structures. The complexes, anionic ligand-coordinated species, with known $(d_{xz})^1(d_{yz})^1(d_{xy})_2(d_z^2)^1(d_z^2)^1(d_{x^2-y^2})^1$configuration have significantly larger iron atom displacements and equatorial Fe-$N_p$bonds.[4] It can be explained that, with more d_{xy}character, spin-orbit coupling will mix in $d_{x^2-y^2}$character more strongly into the doubly occupied orbital for these other iron(II) species than for the imidazole derivatives. The electrostatic repulsion of the in-plane orbital by the negative charge of the pyrrole nitrogens is thus expected to increase the magnitude of the iron atom displacement from the porphyrin plane with a concomitant increase in the value of the Fe-N^pbond distances in comparison to the imidazole-ligated systems.

Although the quadrupole splitting is in principle directly correlated with the detailed structure of the complex,[42] a comparison of the ΔE_Qvalues with the respective structure does not yet suggest a general correlation. Comparing the values for the 1,2-dimethylimidazole complexes with the 2-methylimidazole complexes suggests that the latter have a smaller absolute value for OEP, TTP and T*p*-OCH_3PP derivatives. There may thus be a weak correlation between conformations and quadrupole splitting values.

Summary. Structural studies of two new high-spin iron(II) octaethylporphyrinates undertaken in this investigation show that they have common features to those in tetraarylporphyrinates, such as an expanded porphinato core, large equatorial Fe-$N_p$bond distances and a significant out-of-plane displacement of the iron(II) atom. Both OEP complexes have core doming as the dominant deformation. But there are a number of di ering core conformations observed for all discussed structures, which indicates that there is not a *single* preferred conformation for imidazole-ligated high-spin iron(II) complexes. The di erent core

conformations for di erent crystalline forms of TPP complexes suggest that solid-state packing and solvents in the solid state will also influence the core conformation. Other weak interactions in the solid state, such as π-π interaction and hydrogen bonding, will be other possible factors. Mössbauer studies reveal that the two OEP derivatives have the same behavior as those of tetraaryl derivatives, negative quadrupole splitting values and relative large asymmetry parameters. Both the structures and Mössbauer spectroscopy suggest high-spin iron(II) porphyrinates can be divided into two classes of electron configurations with significantly di erent geometric structures. The anionic ligand coordinated species have the $(d_{xy})^2(d_{xz})^1(d_{yz})^1(d_{z^2})^1(d_{x^2-y^2})^1$ground state, while these imidazole-ligated porphrinates have the ground state with a hybrid orbital comprised of the two axial dπorbitals, with a significant d_{xy}contribution. These features could be importantfor the biological function of heme proteins, such as reversible O_2binding.

Supplementary Material

Refer to Web version on PubMed Central for supplementary material.

Acknowledgments

We thank the National Institutes of Health for support of this research under Grant GM-38401. We thank the NSF for X-ray instrumentation support through Grant CHE-0443233. We thank A. Beatty for early assistance with X-ray data collection.

References and Notes

(1). Perutz MF. Nature 1970;228:226.

(2). Perutz MF. Nature 1972;237:495. [PubMed: 12635193]

(3). Perutz MF, Fermi G, Luisi B, Shaanan B, Liddington RC. Acct. Chem. Res 1987;20:309.

(4). Hu C, Roth A, Ellison MK, An J, Ellis CM, Schulz CE, Scheidt WR. J. Am. Chem. Soc 2005;127:5675. [PubMed: 15826208]

(5). Ellison MK, Schulz CE, Scheidt WR. Inorg. Chem 2002;41:2173. [PubMed: 11952371]

(6). Jameson GB, Molinaro FS, Ibers JA, Collman JP, Brauman JI, Rose E, Suslick KS. J. Am. Chem. Soc 1980;102:3224.

(7). Momenteau M, Scheidt WR, Eigenbrot CW, Reed CA. J. Am. Chem. Soc 1988;110:1207.

(8). The following abbreviations are used in this paper: Porph, a generalized porphyrin dianion; OEP, dianion of octaethylporphyrin; *Tp*-OCH^3PP, dianion of *meso*-tetra-*p*-methoxyphenylporphyrin; TPP, dianion of *meso*-tetraphenylporphyrin; TTP, dianion of *meso*-tetratolylporphyrin, TpivPP, dianion of α,α,α,α-tetrakis(*o*-pivalamidophenyl)-porphyrin; Piv_2C_8P, dianion of α, α,5,15-[2,2'-(octanediamido)diphenyl]- α, α,10-20-bis(o-pivalamidophenyl)porphyrin; Mb, myoglobin; Hb, hemoglobin; Im, generalized imida- zole; RIm, generalized hindered imidazole; HIm, imidazole; 1-MeIm, 1-methylimidazole; 2-MeHIm, 2-methylimidazole; 1,2-Me_2Im, 1,2-dimethylimidazole; N_p, porphyrinato nitrogen; Ct, the center of four porphyrinato nitrogen atoms; EPR, electron paramagnetic resonance; *sad*; saddling; *ruf*, ru ing; *dom*, doming; *wav*, waving; *pro*, propellering.

(9). Rovira C, Kunc K, Hutter J, Ballone P, Parrinello M. J. Phys. Chem. A 1997;101:8914.

(10). Kozlowski PM, Spiro TG, Zgierski MZ. J. Phys. Chem. B 2000;104:10659.

(11). Liao M-S, Scheiner S. J. Chem. Phys 2002;116:3635.

(12). Ugalde JM, Dunietz B, Dreuw A, Head-Gordon M, Boyd RJ. J. Phys. Chem. A 2004;108:4653.

(13). (a) Adler AD, Longo FR, Kampus F, Kim J. J. Inorg. Nucl. Chem 1970;32:2443.Buchler, JW. Porphyrins and Metalloporphyrins. Smith, KM., editor. Elsevier Scientific Publishing; Amsterdam, The Netherlands: 1975. Chapter 5

(14). (a) Fleischer EB, Srivastava TS. J. Am. Chem. Soc 1969;91:2403. (b) Ho man AB, Collins DM, Day VW, Fleischer EB, Srivastava TS, Hoard JL. J. Am.Chem. Soc 1972;94:3620. [PubMed: 5032963]

(15). Sheldrick G. M. Acta Crystallogr 1990;A46:467.

(16). Sheldrick, GM. Program for the Refinement of Crystal Structures. Universität Göttingen; Germany: 1997.

(17). The conventional *R*-factors $R_1$are based on F , with F set to zero for negative$F^2 > 2\sigma(F^2)$ was used only for calculating R^1. *R*-factors based on F^2(wR^2) are statistically about twice as large as those based on F , and *R*-factors based on ALL data will be even larger.

(18). Sheldrick, GM. Program for Empirical Absorption Correction of Area Detector Data. Universität Göttingen; Germany: 1996.

(19). Collman, JP.; Kim, N.; Hoard, JL.; Lang, G.; Radonovich, LJ.; Reed, CA. 167th National Meeting of the American Chemical Society; Los Angeles, CA. April 1974; Washington, D. C.: American Chemical Society; Abstracts of PapersINOR 29

(20). Hu C, Noll BC, Schulz CE, Scheidt WR. J. Am. Chem. Soc 2005;127:15018. [PubMed: 16248628]

(21). Mandon D, Ott-Woelfel F, Fischer J, Weiss R, Bill E, Trautwein AX. Inorg. Chem 1990;29:2442.

(22). Schappacher M, Ricard L, Weiss R, Montiel-Montoya R, Gonser U, Bill E, Trautwein AX. Inorg. Chim. Acta 1983;78:L9.

(23). Nasri H, Fischer J, Weiss R, Bill E, Trautwein AX. J. Am. Chem. Soc 1987;109:2549.

(24). Caron C, Mitschler A, Riviere G, Schappacher M, Weiss R. J. Am. Chem. Soc 1979;101:7401.

(25). Steffen, WL.; Chun, HK.; Hoard, JL.; Reed, CA. 175th National Meeting of the American Chemical Society; Anaheim, CA; March, 1978; Washington, D. C.: American Chemical Society; Abstracts of Papers1978 INOR 15

(26). Reed CA, Mashiko T, Scheidt WR, Spartalian K, Lang G. J. Am. Chem. Soc 1980;102:2302.

(27). Collman JP, Reed CA. J. Am. Chem. Soc 1973;95:2048. [PubMed: 4689928]

(28). Scheidt WR, Reed CA. Chem. Rev 1981;81:543.

(29). Scheidt WR, Lee Y. J. Struct. Bonding (Berlin) 1987;64:1.

(30). Scheidt, WR.; Gouterman, M. Iron Porphyrins. Lever, ABP.; Gray, HB., editors. Addison-Wesley; Reading, MA: 1983. p. 89Part One

(31). Sun, L.; Shelnutt, JA. http://jasheln.unm.edu.

(32). Jentzen W, Ma J-G, Shelnutt JA. Biophys. J 1998;74:753. [PubMed: 9533688]

(33). Kent TA, Spartalian K, Lang G, Yonetani T, Reed CA, Collman JP. Biochem. Biophys. Acta 1979;580:245. [PubMed: 518901]

(34). Debrunner, PG. Iron Porphyrins. Lever, ABP.; Gray, HB., editors. VCH Publishers Inc.; New York: 1983. Part 3Chapter 2.

(35). Schappacher M, Ricard L, Fisher J, Weiss R, Montiel-Montoya R, Bill E. Inorg. Chem 1989;28:4639.

(36). Shaevitz BA, Lang G, Reed CA. Inorg. Chem 1988;27:4607.

(37). Bominaar EL, Ding X, Gismelseed A, Bill E, Winkler H, Trautwein AX, Nasri H, Fisher J, Weiss R. Inorg. Chem 1992;1(3):1845.

(38). Kent TA, Spartalian K, Lang G, Yonetani T. Biochem. Biophys. Acta 1977;490:331. [PubMed: 836876]

(39). Kent TA, Spartalian K, Lang G. J. Chem. Phys 1979;71:4899.

(40). Eicher H, Trautwein A. J. Chem. Phys 1969;50:2540. [PubMed: 5779587]

(41). Schulz, CE.; Scheidt, WR. work in progress.

(42). Zhang Y, Mao J, Oldfield E. J. Am. Chem. Soc 2002;124:7829. [PubMed: 12083937]

Figure 1.
ORTEP diagram of [Fe(OEP)(1,2-Me_2Im)]. The single orientation of the (ordered) imidazole ligand is shown. The hydrogen atoms of the porphyrin ligand have been omitted for clarity. 50% probability ellipsoids are depicted.

Figure 2.
ORTEP diagram of [Fe(OEP)(2-MeHIm)]. The major orientation (75%) of the imidazole ligand is shown. The hydrogen atoms of the porphyrin ligand have been omitted for clarity; the hydrogen atoms of the imidazole ligand are shown. 50% probability ellipsoids are depicted.

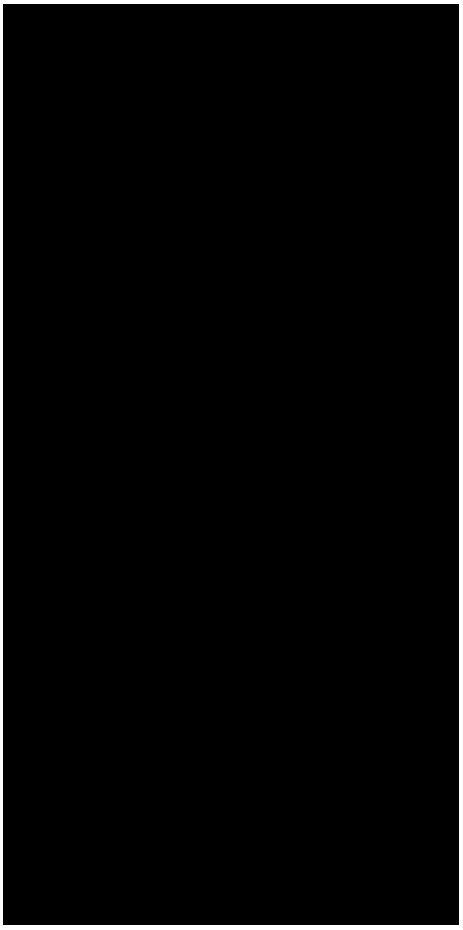

Figure 3.

Formal diagrams of the porphyrinato cores of (top to bottom) a) [Fe(OEP)(1,2-Me_2Im)], b) [Fe- (OEP)(2-MeHIm)], c) [Fe(TPP)(2-MeHIm)].[19] Illustrated are the displacements of each atom from the mean plane of the 24-atom core in units of 0.01 Å. Positive values of displacement are toward the imidazole ligand. The diagrams also show the orientation of the imidazole ligand with respect to the atoms of the porphyrin core. The location of the methyl group at the 2-carbon position is represented by the circle.

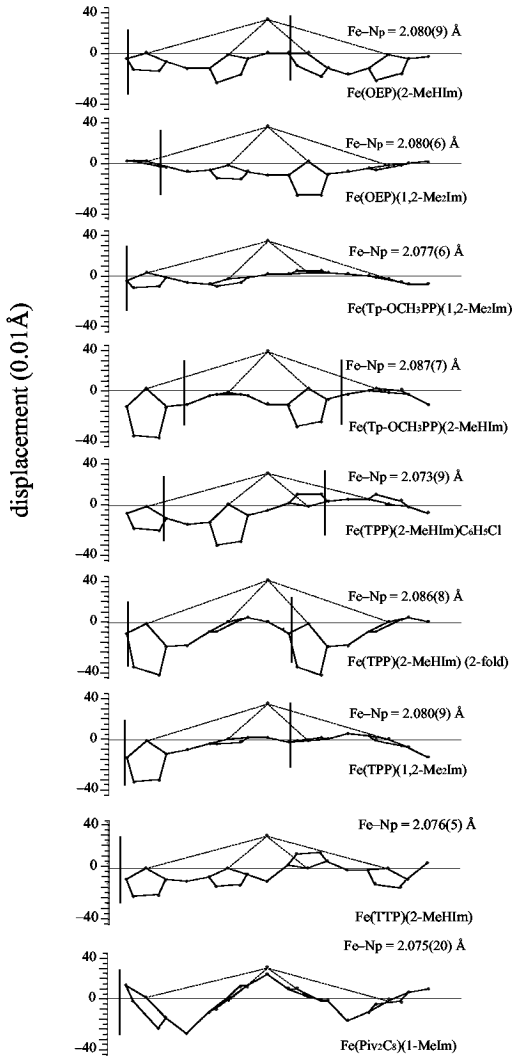

Figure 4.

Diagrams illustrating the core conformation and iron displacement for nine known imidazole-ligated high-spin iron(II) porphyrinates. The displacement of the iron and the atoms of the porphyrin core from the mean plane defined by the four pyrrole nitrogen atoms is given. The position of the imidazole ligand with respect to directions defined by the Fe-$N_p$directions is shown.

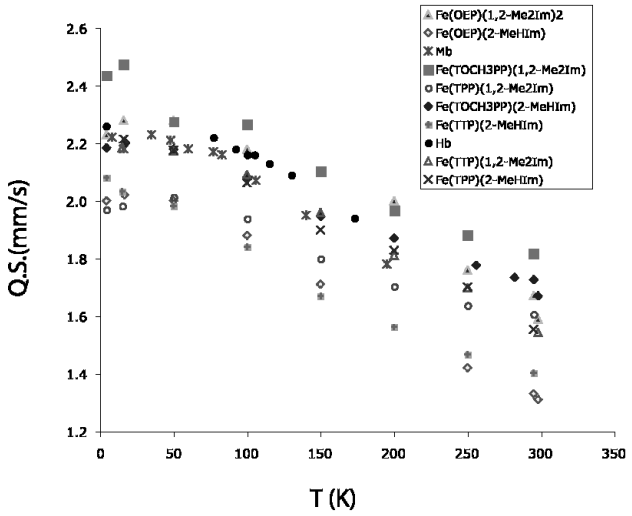

Figure 5.
Plot illustrating the temperature-depedent quadrupole splitting values in the Mössbauer data.

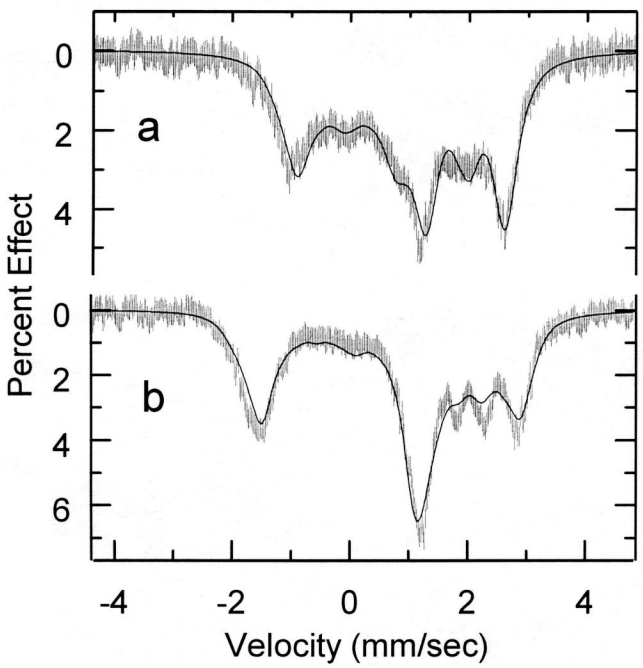

Figure 6.
Figure illustrating the fits to the Mössbauer data obtained at 9 T. Spectrum a) is that obtained for [Fe(OEP)(2-MeHIm)], spectrum b) that for [Fe(OEP)(1,2-Me_2Im)].

Table 1.

Crystallographic Details for the two Structures

	[Fe(OEP)(1,2-Me_2Im)]	**[Fe(OEP)(2-MeHIm)]**
formula	$C_{41}H_{52}FeN_6$. $0.97C_6H_5CH_3$	$C_{40}H_{50}FeN_6.C_6H_5CH_3$
FW	776.87	762.84
a, Å	20.2439(15)	12.6335(6)
b, Å	19.7769(14)	12.9323(6)
c, Å	10.1528(7)	13.5470(7)
α	90	82.285(5)
β, deg	91.651(2)	75.039(2)
γ	90	71.063(2)
V , $Å^3$	4063.1(5)	2019.47(17)
Z	4	2
space group	P 2_1/c	P1
Dc, g/cm^3	1.265	1.255
F (000)	1657	816
μ, mm^{-1}	0.413	0.414
crystal dimens, mm	0.2 × 0.1 × 0.05	0.46 × 0.11 × 0.06
absorption correction	SADABS	
radiation, MoKα, ƛ	0.71073 Å	
T , K	100(2)	100(2)
total data collected	32777	30390
unique data	7181 (R_{int} = 0.0575)	8143 (R_{int} = 0.0330)
unique obsd data [I > 2 σ(I)]	5839	6676
refinement method	on F^2 (SHELXL)	
final R indices [I > 2 σ(I)]	R_1 = 0.0600, wR_2 = 0.1556	R_1 = 0.0467, wR_2 = 0.1294
final R indices [for all data]	R_1 = 0.0750, wR_2 = 0.1174	R_1 = 0.0590, wR_2 = 0.1409

Table 2.

Selected Bond Distances (Å) and Angles (deg) for [FeOEP)(Im)] and Related Species[a]

Complex[b]	Fe-N_p[c,d]	Fe-L_{Ax}[d]	ΔN_4[d,e]	Δ,[df]	Ct…N[d]	Fe-N-C,[gh]	Fe-N-C,[gi]	θ,[gj]	Φ,[gk]	ref
				Iron(II)						
[Fe(OEP)(1,2-Me_2Im)]	2.080 (6)	2.171 (3)	0.37	0.45	2.047	132.7 (3)	121.4 (2)	3.8	10.5	tw
[Fe(OEP)(2-MeHIm)]	2.077 (7))	2.135 (3)	0.34	0.46	2.049	131.3 (3)	122.4 (3)	6.9	19.5	tw
average of the two	2.078 (2)	2.153 (25)	0.36	0.46	2.048 (1)	132.0 (10)	121.9 (7)	5.4 (22)		
[Fe(TPP)(1,2-Me_2Im)]	2.079 (8)	2.158 (2)[l]	0.36	0.42	2.048	129.3 (2)	124.9 (2)	11.4	20.9	4
[Fe(TTP)(2-MeHIm)]	2.076 (3)	2.144 (1)	0.32	0.39	2.050	132.8 (1)	121.4 (1)	6.6	35.8	4
[Fe(Tp-OCH_3PP)(2-MeHIm)]	2.087 (7)	2.155 (2)[l]	0.39	0.51	2.049	130.4 (2)	123.4 (2)	8.6	44.5	4
[Fe(Tp-OCH_3PP)(1,2-Me_2Im)]	2.077 (6)	2.137 (4)	0.35	0.38	2.046	131.9 (3)	122.7 (3)	6.1	20.7	4
[Fe(TPP)(2-MeHIm)](2-fold)	2.086 (8)	2.161 (5)	0.42	0.55	2.044	131.4 (4)	122.6 (4)	10.3	8.6	19
[Fe(TPP)(2-MeHIm)]·1.5C_6H_5Cl	2.073 (9)	2.127 (3)[l]	0.32	0.38	2.049	131.1 (2)	122.9 (2)	8.3	24.0	5
average of the six (tetraaryls)	2.080 (6)	2.147 (13)	0.36(4)	0.44 (7)	2.048 (2)	131.2 (10)	123.0 (11)	8.6 (20)		
average of the eight (all)	2.080 (5)	2.147 (16)	0.36(3)	0.44 (6)	2.048 (2)	131.4 (12	122.7 (11	7.8 (24)		
[Fe(TpivPP)(2-MeHIm)]	2.072 (6)	2.095 (6)	0.40	0.43	2.033	132.1 (8)	126.3 (7)	9.	22.8	6
[Fe(Piv_2C_8P)(1-MeIm)	2.075 (20	2.13 (2)	0.31	0.34	2.051	126.5	120.4	5.0	34.	7
[K(222)][Fe(OEP)(2-$MeIm^-$)]	2.113 (4)	2.060 (2)	0.56	0.65	2.036	136.6 (2)	120.0 (2)	3.6	37.4	20
[K(222)][Fe(TPP)(2-$MeIm^-$)]	2.118 (13)	1.999 (5)	0.56	0.66	2.044	129.6 (3)	126.7 (3)	9.8	23.4	20
		2.114 (5)				133.6 (4)	121.9 (4)	6.5	21.6	
[Fe(TpivPP)(2-$MeIm^-$)]$^-$	2.11 (2)	2.002 (15)	0.52	0.65	2.045	NR[m]	NR	5.1	14.7	21
[Fe(TpivPP)Cl]$^-$	2.108 (15)	2.301 (2)[n]	0.53	0.59	2.040	-	-	-	-	22
[Fe(TpivPP)(O_2CCH_3)]$^-$	2.107 (2)	2.034 (3)[o]	0.55	0.64	2.033	-	-	-	-	23
[Fe(TpivPP)(OC_6H_5)]$^-$	2.114 (2)	1.937 (4)[o]	0.56	0.62	2.037	-	-	-	-	23
[Fe(TpivPP)(SC_6HF_4)]$^-$	2.076 (20)	2.370 (3)[p]	0.42	NR	2.033	-	-	-	-	22
[Fe(TPP)(SC_2H_5)]$^-$	2.096 (4)	2.360 (2)[p]	0.52	0.62	2.030	-	-	-	-	24
[Fe(TPP)(1-$MeIm)_2$][q]	1.997 (4)	2.014 (5)	0.0[r]	0.0[r]	1.997	128.2	128.3	1.1	14.7	25
[Fe(TPP)($THF)_2$]	2.057 (4)	2.351 (3)[s]	0.0[r]	0.0[r]	2.057	-	-	-	-	26

[a] Estimated standard deviations are given in parentheses.

[b] Unless noted otherwise, complex is high spin.

[c] Averaged value.

[d] in Å.

[e] Displacement of iron from the mean plane of the four pyrrole nitrogen atoms.

[f] Displacement of iron from the 24-atom mean plane of the porphyrin core.

[g] Value in degrees.

[h] 2-carbon, sometimes methyl substituted.

[i] Imidazole 4-carbon.

[j] Off-axis tilt (deg) of the Fe-NIm bond from the normal to the porphyrin plane.

[k] Dihedral angle between the plane defined by the closest N_p-Fe-N_{im} and the imidazole plane in deg.

[l] Major imidazole orientation.

[m] Not reported.

[n] Chloride.

[o] Anionic oxygen donor.

[p] Thiolate.

[q] Low Spin.

[r] Six-coordinate; required to be zero by symmetry.

[s] Neutral oxygen donor.

Table 3.

Out-of-Plane Displacements(Å)of the Minimal Basis for the X-ray Crystal Structures of Five-Coordinate High-Spin Iron(II) Porphyrinates

porphyrin	Doop[a]	δ_{oop}[b]	sad	ruf	dom	wav (x)	wav (y)	pro	ΔN_4[c]	Δ[d]	ref
[Fe(OEP)(2-MeHIm)]	0.437	0.012	0.112	0.216	-0.356	0.066	-0.004	-0.018	0.34	0.46	tw
[Fe(OEP)(1,2-Me2Im)]	0.282	0.013	-0.085	-0.052	-0.225	0.014	0.137	-0.006	0.37	0.45	tw
[Fe(TPP)(2-MeHIm)(2-fold)]	0.872	0.018	-0.672	0.336	-0.444	-0.000	-0.000	-0.024	0.42	0.55	19
[Fe(T_p-OCH_3PP)(2-MeHIm)]	0.652	0.024	-0.546	0.057	0.350	-0.039	0.014	-0.004	0.39	0.51	4
[Fe(TPP)(2-MeHIm)]	0.310	0.020	-0.119	0.012	0.180	0.200	-0.095	0.012	0.32	0.38	19
[Fe(TTP)(2-MeHIm)]	0.302	0.014	0.155	0.055	0.204	0.147	-0.024	0.006	0.32	0.39	4
[Fe(TPP)(1,2-Me2Im)]	0.362	0.019	0.265	-0.077	-0.202	-0.116	-0.005	0.008	0.36	0.42	4
[Fe(T_p-OCH_3PP)(1,2-Me_2Im)]	0.116	0.014	-0.070	-0.018	0.082	-0.038	0.007	-0.004	0.35	0.38	4
[Fe(Piv_2C_8P)(1-MeIm)]	0.607	0.036	-0.026	-0.594	-0.077	-0.086	-0.017	-0.040	0.31	0.34	7

[a] Observed total distortion.

[b] The mean deviation as a measurem of the goodness-of-fit.

[c] Displacement of iron fromthe mean plane of the four pyrrole nitrogen atoms.

[d] Displacement of iron from the 24-atom mean plane

Table 4.

Mössbauer Parameters for Five-Coordinate, High-Spin Imidazole-Ligated Iron(II) Porphyrinates and Hb and Mb

Complex	ΔE_Q [a]	δ_{Fe} [a]	η	Γ [b]	T, K	ref.
[Fe(OEP)(1,2-Me_2Im)]	-2.19	0.92	0.43	0.38	4.2	tw
[Fe(OEP)(2-MeHIm)]	-1.94	0.93	0.26	0.42	4.2	tw
[Fe(Tp-OCH_3PP)(1,2-Me_2Im)]	-2.44	0.95	0.65	0.46	4.2	4
[Fe(Tp-OCH_3PP)(2-MeHIm)]	-2.18	0.94	0.58	0.53	4.2	4
[Fe(TPP)(1,2-Me_2Im)]	-1.93	0.92	0.2	0.44	4.2	4
[Fe(TPP)(2-MeHIm)]	-1.96	0.86	0.55	0.6	4.2	4
[Fe(TTP)(2-MeHIm)]	-1.95	0.85	0.1	0.42	4.2	4
[Fe(TTP)(1,2-Me_2Im)]	-2.06	0.86	0.04	0.43	4.2	4
[Fe(TPP)(2-MeHIm)]	-2.40	0.92	0.8	0.50	4.2	5
[Fe(TPP)(2-MeHIm)(2-fold)	-2.28	0.93	0.8	0.31	4.2	33
[Fe(TPP)(1,2-Me_2Im)]	-2.16	0.92	0.7	0.25	4.2	33
[Fe((Piv_2C_8P)(1-MeIm)]	-2.3[c]	0.88		0.40	4.2	7
Hb	-2.40	0.92	0.7	0.30	4.2	33
Mb	-2.22	0.92	0.7	0.34	4.2	33
[Fe(OEP)(2-$MeIm^-$)]	+3.71	1.0	0.22	0.29	4.2	20
[Fe(TPP)(2-$MeIm^-$)]	+3.60	1.00	0.02	0.33	4.2	20
[Fe(TpivPP)(SC_2H_5]$^-$	+2.18	0.83	0.80	0.30	4.2	35
[Fe(OC_6H_5)(TPP)]$^-$	+4.01	1.03	0	0.25	4.2	36
[Fe(O_2CCH_3)(TpivPP)]$^-$	+4.25	1.05	0	0.30	4.2	37
[Fe(OCH_3)(TpivPP)]$^-$	+3.67[d]	1.03		0.40	4.2	23
[Fe(OC_6H_5)(TpivPP)]$^-$	+3.90 [d]	1.06		0.38	4.2	23
[Fe(TpivPP)(2-MeIm)]$^-$	+3.51[d]	0.97			77	21
[Fe(TpivPP)(SC_6HF_4)] [NaC12H24O6]	+2.38[d]	0.84		0.28	4.2	35
[Fe(TpivPP)(SC_6HF_4)][NaC222]	+2.38[d]	0.83		0.32	4.2	35
[Fe(TpivPP)Cl]$^-$	+4.36[d]	1.01		0.31	77	22

[a] mm/s.

[b] Line width, FWHM.

[c] Sign not determined experimentally, presumed negative.

[d] Sign not determined experimentally, presumed positive.